ACS OMEGA

Article

Cite This: ACS Omega 2020, 5, 674−682

Construction and Evaluation of Collagen-Based Corneal Grafts Using Polycaprolactone To Improve Tension Stress

Xiaomin Sun,[†,‡,§,∥,⊥] Xiangjing Yang,[†,‡,§,∥,⊥] Wenjing Song,*[,†,‡,§,∥,⊥] and Li Ren*[,†,‡,§,∥,⊥,#,¶]

[†]School of Materials Science and Engineering, [‡]Key Laboratory of Biomedical Engineering of Guangdong Province, [§]Key Laboratory of Biomedical Materials and Engineering of the Ministry of Education, and [∥]Innovation Center for Tissue Restoration and Reconstruction, South China University of Technology, Guangzhou 510006, P. R. China

[⊥]National Engineering Research Center for Tissue Restoration and Reconstruction, Guangzhou 510006, P. R. China

[#]Sino-Singapore International Joint Research Institute, Guangzhou 510555, P. R. China

[¶]Guangzhou Regenerative Medicine and Health Guangdong Laboratory, Guangzhou 510005, P. R. China

ABSTRACT: The emergence of innovative surgical procedures using partial thickness corneal transplant has created a need for the development of corneal grafts to replace pathologic corneal tissue. Corneal repair materials have been successfully prepared in the past 10 years, but they were difficult to be used in clinics because of the unbearable tension caused by interrupted suture during routine surgery. However, polycaprolactone (PCL), a medical polymer material, can solve this problem. Therefore, a hierarchical collagen (Col)-based corneal graft with curvature, consisting of a transparent core part composed of collagen in the center and a mechanically robust fixed part containing collagen and polycaprolactone in the edge, was used as a potential corneal graft for corneal repair and regeneration in this study. The hierarchical collagen-based corneal grafts [collagen−polycaprolactone (Col−PCL) membranes] that are capable of mimicking the native cornea were developed based on chemical and thermal crosslinking mechanisms. The water adsorption of Col−PCL membranes could reach over 80% similar to that of human cornea, and its swelling could reach over 400%. More importantly, the formed Col−PCL membranes could resist a larger tensile strength (1.1 ± 0.03 MPa) before rupturing in comparison with pure collagen membranes and polycaprolactone membranes. Furthermore, the biodegradable Col−PCL membranes could facilitate cell adhesion and proliferation as well as cell migration (exhibiting epithelial wound coverage in <5 days), which showed promise as corneal grafts for cornea tissue engineering.

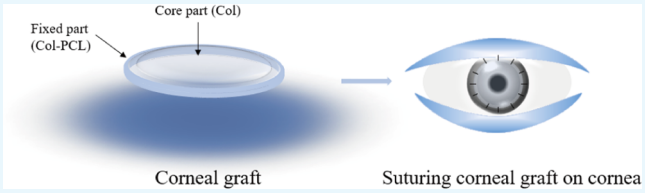

1. INTRODUCTION

Cornea is a delicate tissue that are crucial for normal vision. Different from many other tissues, cornea is an avascular, hierarchical, and transparent tissue on the surface of human eyes.[1] Damage from mechanical, thermal, or chemical injuries and microbial infections frequently leads to the dysfunction of cornea, resulting in the appearance of grayish-white opacification in the transparent cornea, vision loss, and even blindness.[2−4] At present, the donor corneal graft is a widely accepted therapeutic method because of its accessibility and immune privilege.[1] However, donors are inadequate and difficult to match patients.[5] The emergence of innovative surgical procedures using partial thickness corneal transplants has created a need for the development of corneal grafts to replace pathologic corneal tissue. This procedure has been called anterior lamellar keratoplasty (ALKP).[6−8] Therefore, many researchers have attempted to develop corneal grafts using natural macromolecule materials to replace pathologic corneal tissue via ALKP.[1,9] The corneal stroma, which accounts for approximately 90% of the cornea, mainly composes of aligned collagen (Col) I fibrils and quiescent keratocytes.[10−12] Bionic corneal structures are the key to the development of successful corneal products. In addition, the cornea repair materials should possess good biocompatibility and nutrition permeability, appropriate optical performance and mechanical strength.[13−15] Although many cornea repair materials have been successfully obtained in a variety of ways,[1,9,14−19] the main problem is that they are difficult to apply in the clinical suture.

Collagen (Col), a natural biopolymer, is used widely as a biomaterial in medical areas, with biocompatibility, biodegradability, and biological activity,[20−24] which makes Col possible to be excellent candidates for the tissue repair material. Meanwhile, it is also the main component of corneal stroma. However, the poor mechanical toughness and elasticity limited its clinical application in our previous work.[16,17,25,26] Therefore, Col is often accompanied by other materials to counteract its poor mechanical properties. Another material which was successfully used in tissue repair and functional reconstruction, showing good results, was polycaprolactone (PCL).[27−31] PCL is a hydrophobic and semicrystalline polymer, exhibiting more advantages, including versatile mechanical performance, slower

Received: October 5, 2019
Accepted: December 18, 2019
Published: January 2, 2020

DOI: 10.1021/acsomega.9b03297
ACS Omega 2020, 5, 674−682

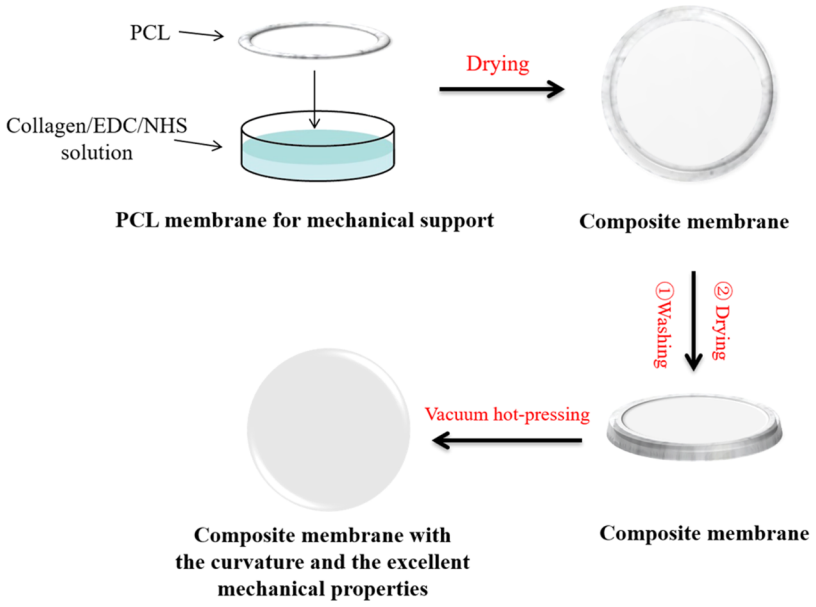

Figure 1. Preparation process of Col–PCL composite membranes.

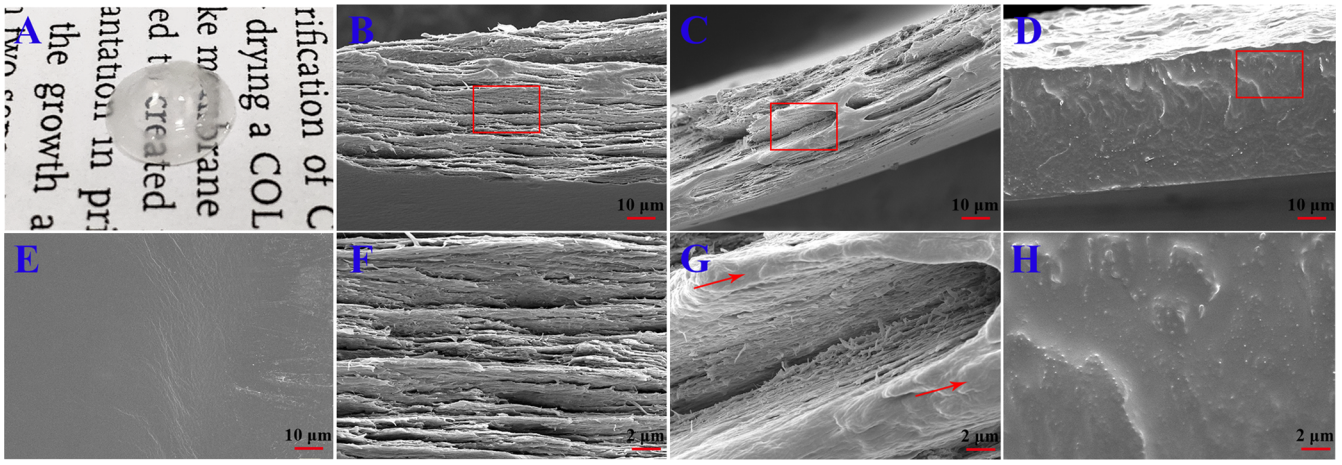

Figure 2. Macroscopic and microscopic morphology of the membranes. (A) Macroscopic of the Col–PCL membrane. Scanning electron microscopy (SEM) images from (E) surface of the Col–PCL membrane and longitudinal section of (B, F) Col, (C, G) Col–PCL, and (D, H) PCL membranes [(B–E) bar = 10 μm; (F–H) bar = 2 μm]. Red arrows show the reconstructive PCL.

degradation rate, and lesser inflammation.[27,32,33] These advantages have a potential significance on the biomedical applications of PCL, such as sutures and fixation devices.[34−37] However, it still has its own limitations, such as high hydrophobicity, poor cell attachment, and proliferation. To solve these limitations, Ma's team reported on biocomposites of both synthetic and natural polymers that can be identified and metabolized in the biological environment.[38]

In previous work, collagen as a cornea repair material could hardly bear interrupted stitching during routine surgery,[39,40] which limited its clinical application. In this study, our aim is to solve the problem of low mechanical strength and difficult suture in cornea transplant operation. Col–PCL membranes were prepared using chemical crosslinking and thermal crosslinking methods during membrane formation, consisting of a transparent core part composed of collagen in the center and a mechanically robust fixed part containing collagen and PCL in the edge. The fixed part is convenient for suturing during operation. After the preparation of Col–PCL membranes, the physical properties of the membranes were characterized in optical transparency, water content, and tensile strength. The in vitro cytocompatibility of the membranes to human corneal epithelial cells (HCECs) was evaluated. Finally, the in vitro ability of re-epithelialization has been examined using an ex vivo corneal graft culture model.

2. RESULTS AND DISCUSSION

2.1. Macroscopic and Microscopic Morphology Characteristics. Because of the special structure of corneal stroma, designing corneal structure is the key to the development of a successful corneal product to repair a corneal anterior lamellar defect. In this study, a rehydrated Col–PCL composite membrane with curvature and transmittance was successfully prepared (Figure 1) and is shown in Figure 2A. It consisted of a transparent core part composed of collagen in the center and a mechanically robust fixed part containing Col and PCL in the edge. The core part provided optical performance for vision, and the fixed part provided interrupted suture during surgery. Figure 2E shows the surface

DOI: 10.1021/acsomega.9b03297
ACS Omega 2020, 5, 674−682

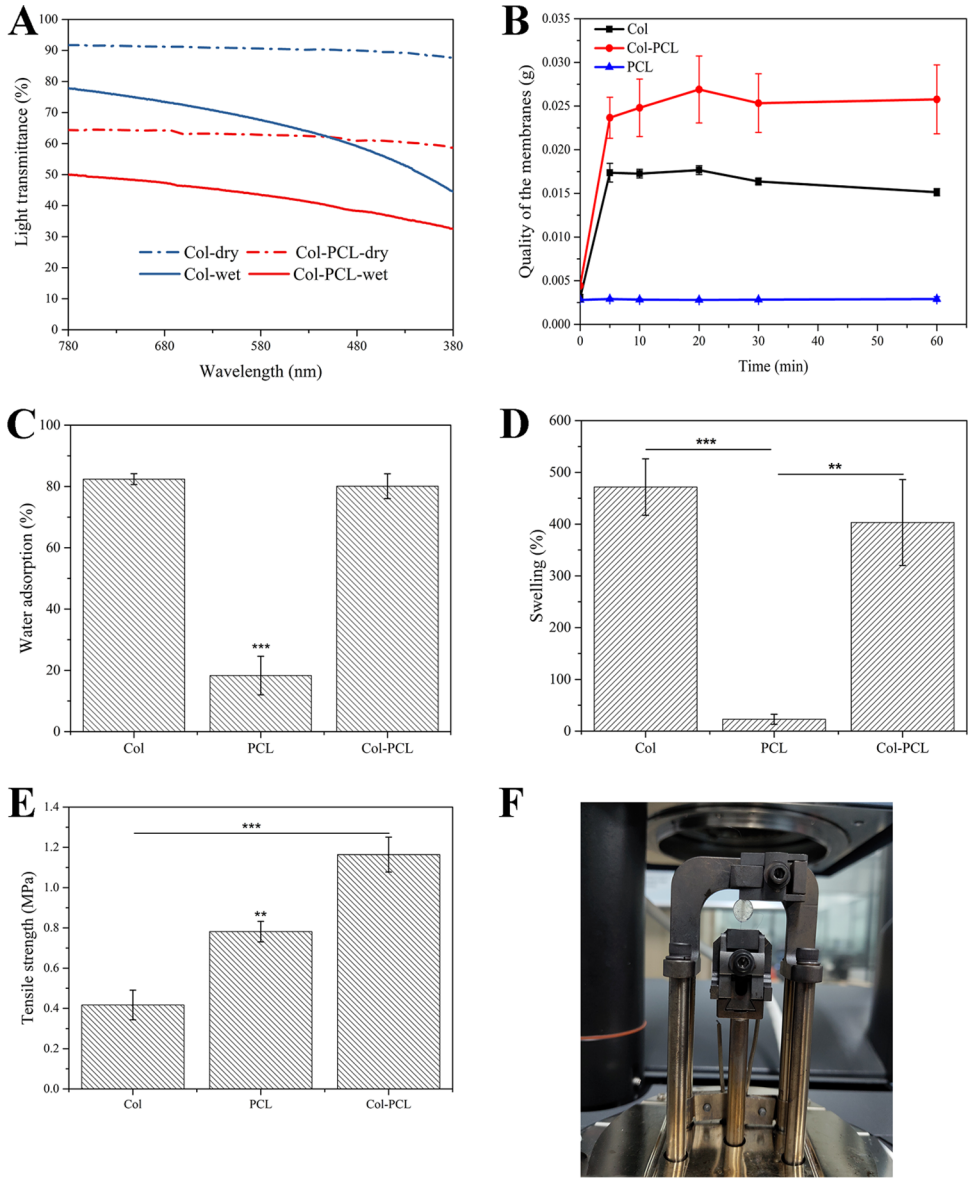

Figure 3. Physical characterization of Col, Col−PCL, and PCL membranes. (A) Light transmission over visible light spectrum (380−780 nm), (B) water saturation {mass (membranes) + mass [weight of absorbed normal saline (NS)]} following the change of time, (C) water adsorption, (D) swelling, and (E) tensile strength of the wet membranes. (F) Simulated tension of suture during surgery to measure suture tension using dynamic mechanical analysis (DMA). Data are means ± standard deviation (SD), $n = 3$, $^{***}p < 0.001$, $^{**}p < 0.01$.

of a dry Col−PCL membrane, which presented a lower and smoother core part composed of Col and a higher and rough fixed part composed of Col−PCL, but the core part and fixed part had the same plane after absorbing water. A lamellar structure similar to native cornea was discovered in Figure 2B,C,F,G. The Col−PCL membrane (Figure 2C,G) had a small amount of reconstructive PCL that showed a dense structure compared to the Col membrane (Figure 2B,F). At 120°, liquid PCL infiltrated into the collagen membrane. The PCL infiltrating into collagen provides mechanical properties for the surgical suture, which is mainly due to the mechanical properties of PCL itself. After returning to room temperature, PCL existed in the form of a reconstructive solid state. Group PCL exposed a dense structure (Figure 2D,H), which was not conducive to air permeability and nutrient transport. Interestingly, the dense structure was similar to where indicated by the red arrow in Figure 2C,G. Although a dense structure similar to PCL appears, it was small and did not affect air permeability and nutrient transport of the material itself. Therefore, a small amount of the reconstructive PCL may be more suitable for this study.

2.2. Physical Characterization. Transparency is critical to the functionality of corneal grafts and is related to the collagen organization, which contributes to the transparency with its water-retaining proteoglycans.[41,42] Clinically, the degree of corneal injury is different for each patient, so corneal grafts should be of different thickness and size for patients to choose. All dry membranes in this study were about 40 ± 5 μm. Col membranes as a positive control represented the core part of the Col−PCL membrane, which had higher transparency values than the fixed part of Col−PCL membranes (Figure 3A). The fixed part of dry Col−PCL membranes with 40 μm thickness was 60% transparent at 780 nm and the fixed part of wet Col−PCL membranes with 400 μm thickness was only

DOI: 10.1021/acsomega.9b03297
ACS Omega 2020, 5, 674−682

42% transparent at 780 nm, because their internal structure was damaged after swelling. Therefore, it is impossible to achieve minimal functional transparency at a thickness of human corneal thickness with these grafts. Importantly, it only provides surgical suture, not vision. However, the core part of Col−PCL membranes was the Col with 40 μm thickness, which was 90% transparent at 780 nm in a dry environment. Within the same 400 μm thickness, wet Col membranes were 78% transparent at 780 nm. The transparency of Col membranes in the visible range was lower than that of native cornea (87%),[43] but it was observed that the transmittance of the membranes increased gradually in our long-term in vivo experiments.

The cornea is a water-bearing tissue with moisture retention capacity. Before surgery, the corneal grafts will be rehydrated until it reaches saturation. After rehydration for 60 min, the quality of PCL membranes remained constant because of its hydrophobicity (Figure 3B); the saturation curves of Col and Col−PCL membranes had a common feature that was oversaturated (10−30 min) before reaching stable saturation (30−60 min). Therefore, the corneal grafts only need to be rehydrated 30 min before surgery. Moreover, quality of Col membranes after rehydration was higher than Col−PCL membranes, which was mainly due to the higher content of Col in Col membranes.

The water adsorption and swelling properties play an important role in maintaining the structural stability of corneal grafts, which is in favor of cell migration, adhesion, and proliferation. To further evaluate the physical properties of Col, Col−PCL, and PCL membranes, water adsorption and swelling were characterized because they can judge the hydrophilic properties of materials. After 24 h of incubation in NS, the water adsorption of Col and Col−PCL membranes could reach over 80%, while those of PCL membranes were only less than 20% (Figure 3C) and there were significant differences between them, but there was no significant difference between Col and Col−PCL. Therefore, Col and Col−PCL membranes demonstrated similar water adsorption to human cornea (78−82%).[15] Furthermore, the swelling of Col, Col−PCL, and PCL membranes was measured under the same conditions. The swelling of Col and Col−PCL membranes could reach over 400%, while those of PCL membranes were only less than 30% (Figure 3D). No significant difference was observed in Col and Col−PCL, but there were significant differences between them and PCL. Therefore, Col−PCL membranes with excellent moisture retention capacity can maintain water balance and provide a water environment for cell adhesion and proliferation.

Besides the above-mentioned transparency and swelling properties, the mechanical properties of corneal grafts also play an important role in surgical suture.[44] Therefore, the mechanical properties were characterized using a method of the simulated tension of suture during surgery. The native corneas usually underwent environmental shear or tensile stress resulting from the blink and the intraocular pressures.[45] Furthermore, surgical implantation of a corneal graft requires tensile strength to support suturelike native tissue. Therefore, the tensile properties of Col−PCL membranes were tested and compared with Col and PCL. An engineered suture pull-out test (Figure 3F) found that Col−PCL membranes could withstand a larger tensile strength (1.1 ± 0.03 MPa) than Col and PCL membranes before rupturing and the differences were significant (Figure 3E). The results showed that the mechanical properties of Col membranes were enhanced by the melted PCL, and the tensile strength of Col−PCL membranes was close to the sum of Col and PCL. Meanwhile, the results suggested that they have the potential to bear routine interrupted suture in clinics.

2.3. In Vitro Degradation. Controllable corneal graft degradation kinetics are also very crucial for the regeneration of cornea. It would be beneficial if the implanted corneal graft is degraded and replaced by normal cornea tissue.[15] Col is usually degraded by collagenase, which is present in tear films.[46] To investigate the degradation time of the prepared corneal grafts in vitro, the membranes were incubated in phosphate-buffered saline (PBS) containing 0.017 ng/mg of collagenase type I at 37 °C. Figure 4 depicts the degradation

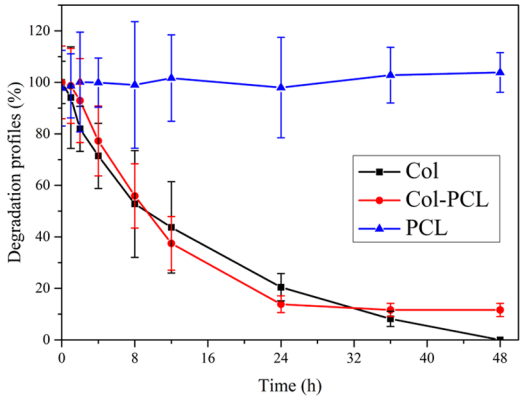

Figure 4. In vitro degradation assessment of Col, Col−PCL, and PCL membranes.

profiles of all membranes (Col, Col−PCL, and PCL) with different incubation times. After continuous incubation for 8 h, the Col membrane lost nearly half of its mass and degraded the most. This may be because the reconstructive PCL prevents the rapid degradation of Col. After 24 h, the mass of Col membranes remained 20.45%, Col−PCL membranes remained 13.86%, and PCL membranes did not change. Col−PCL membranes stabilized in 24 h, and the quality remained unchanged in the following time. Moreover, Col membranes could maintain degradation for 48 h; Col−PCL membranes could maintain degradation for 24 h; and PCL membranes could not degrade. Therefore, the enzymatic degradation of the membranes suggests that PCL with slow degradation is feasible as a fixing part and that may be used for biomedical applications.

2.4. Cell Proliferation and Adhesion. Cell proliferation and adhesion are essential for corneal grafts;[47,48] thus, cell proliferation and adhesion assay were carried out on the as-prepared membranes. A cell counting kit-8 (CCK-8) kit was used to quantificationally estimate the proliferation and adhesion of HCECs as shown in Figure 5A,B. In cell proliferation experiments, the proliferation rate of cells on the three membranes was close to each other after 5 days of culture and there were no significant differences. At day 3, the proliferation rate of cells on PCL membranes was the lowest compared to that of Col and Col−PCL membranes due to the low adhesion rate of PCL. However, the cell proliferation rates of all membranes were lower than that of the control group, because some cells floated on the cell culture plate when planting cells. Moreover, optical density (OD) values increased with the incubation time. To evaluate the cell adhesion of

DOI: 10.1021/acsomega.9b03297
ACS Omega 2020, 5, 674−682

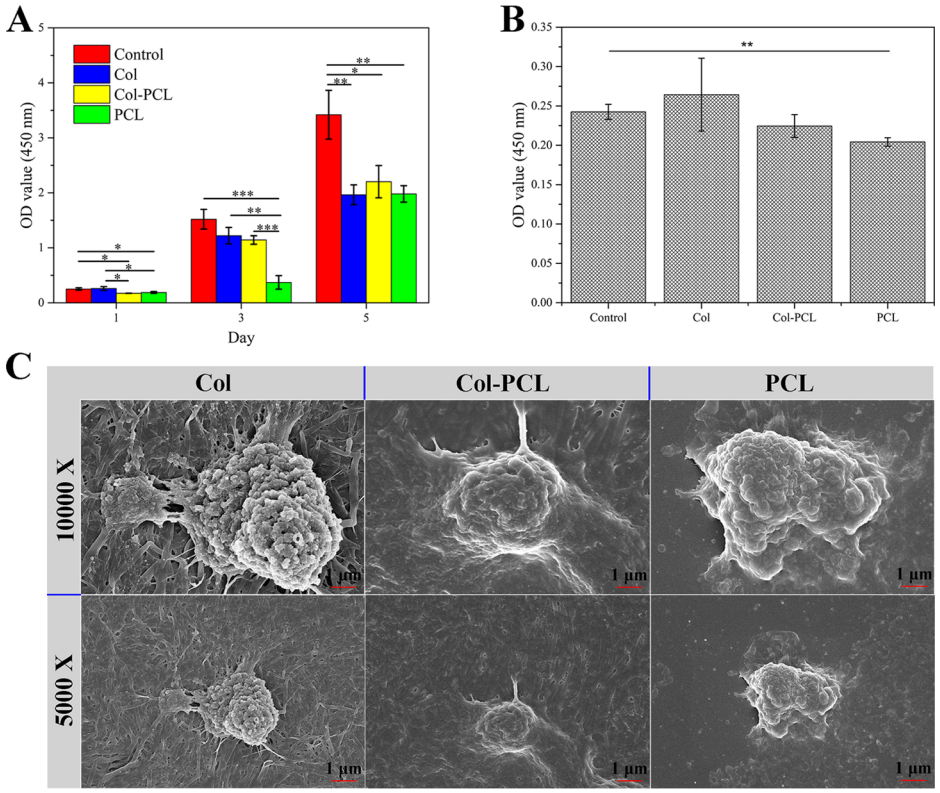

Figure 5. Cell proliferation and adhesion assay of Col, Col−PCL, and PCL membranes. (A) Cell proliferation of Col, Col−PCL, and PCL membranes for day 1, 3, and 5. (B) Number of HCECs adhering to membranes for 1 day. (C) SEM images from HCECs adhering to membranes. Data are means ± SD, $n = 3$, $^{***}p < 0.001$, $^{**}p < 0.01$.

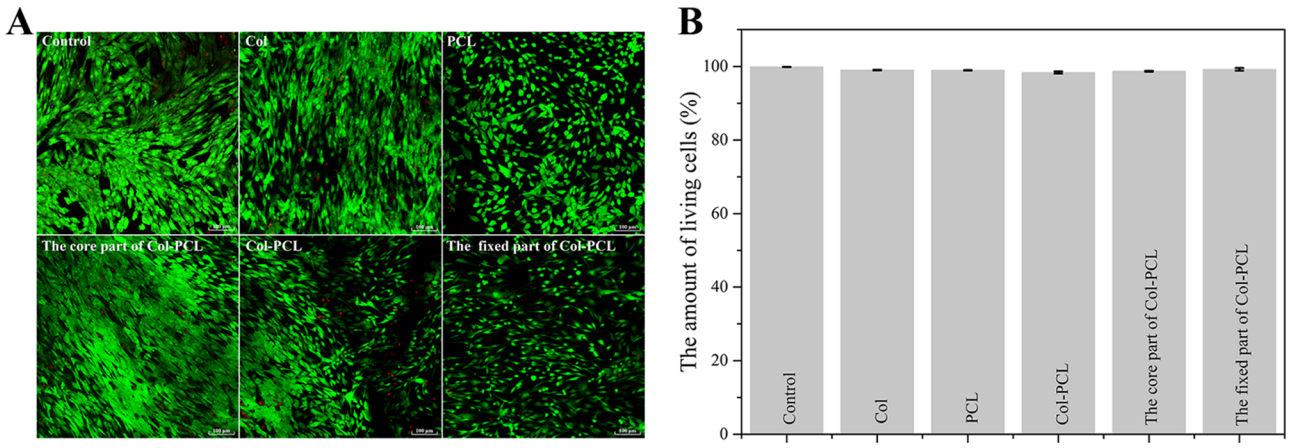

Figure 6. Viability of HCECs on the membranes. (A) Live/dead assay of HCECs stained by calcein-AM/PI. (B) Quantified cell viability using ImageJ software.

Col−PCL membranes, the OD values of HCECs remaining on the membrane after washing with PBS are plotted in Figure 5B. After incubation for 1 day, the cell adhesion on the three membranes was different and there were no significant differences between them. However, there was a significant difference between the control group and PCL membranes. The results indicated that PCL membranes have relatively poor cell adhesion, which is consistent with the results of cell proliferation. To further evaluate cell adhesion of the three membranes, the cell morphology adhered to the membranes was obtained by SEM (Figure 5C). Compared with PCL membranes, HCECs could spread well with a fibroblastic morphology. All of these results were consistent with the quantification of HCECs to estimate their proliferation and adhesion and illustrated the potential use of Col−PCL membranes for tissue engineering applications.

2.5. Live/Dead Cell Viability Assay. Studying the impact of the membrane on HCEC viability is of great interest to biocompatibility of membranes. To perform the assay, HCECs were used to evaluate cell viability on the membranes by means of calcein acetoxymethyl (calcein-AM)/propidium iodide (PI) double staining performed at 5 days (Figure 6). HCECs adhering to the membranes were homogenously distributed and retained high cell viability over 5 days postculture (Figure 6A). In addition, minimal cell death was shown in all groups. At the same magnification, the cell adhesion area on the PCL

DOI: 10.1021/acsomega.9b03297
ACS Omega 2020, 5, 674−682

membrane was significantly smaller than that on Col and Col−PCL membranes. These results were consistent with the cell adhesion experiments in Figure 5B,C. Cell viability in different groups was quantified using ImageJ. All membranes showed nearly 100% cell viability, and there were no significant differences.

2.6. Ex Vivo Cell Migration. Epithelial cells maintain a balance between limbal stem function, tear quantity and quality, eyelid anatomy and function, and corneal sensitivity.[49] Although various corneal materials have been reported to promote corneal tissue repair, challenges remain in epithelialization of corneal grafts. There are also other important differences between in vitro and ex vivo approaches. Compared with the traditional cell culture, the intact eyeball contains several cell types with different properties and functions. It is expected that these cells communicate with each other, thus interactively influencing their behavior during wound healing. This might be mediated via secreted cytokines or proteins. Although ex vivo approaches have the advantage of avoiding painful treatments of animals and have been applied with significant success,[50−52] such an experimental method has the disadvantage of systemic circulation. Even though ex vivo models are limited by clinical transformation, it has also shown the applicability of the cell migration experiment. The migration of HCECs on Col−PCL membranes was assessed on the basis of the ex vivo corneal graft culture model, to ensure that Col−PCL membranes support cell growth and migration without adding any exogenous cells. As shown in Figure 7, a clear corneal defect model was established in ex vivo rabbit eye and the Col−PCL membrane was successfully sutured on the rabbit cornea in the experimental group. On day 3, a larger area of re-epithelization appeared in the Col−PCL membrane compared to the control group. More interestingly, re-epithelialization of Col−PCL membranes completed at 5 days postculture compared to the control group, characterized by fluorescein staining. The results demonstrated that HCECs could migrate and cover over the implant region.

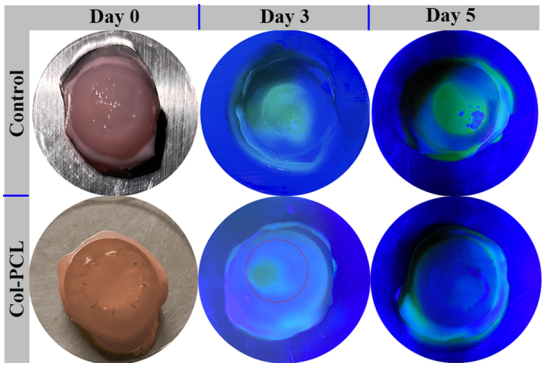

Figure 7. Photograph of fluorescein staining for tracing the process of corneal wound healing over 5 days. Yellow-green staining under blue light indicates regions without epithelial cell coverage.

3. CONCLUSIONS

In conclusion, corneal grafts (Col−PCL membranes) with curvature, transparency, and robust tensile stress were engineered using chemical crosslinking and thermal crosslinking methods during membrane formation. These corneal grafts display a lamellar structure that are capable of simulating the native cornea, which consists of a transparent core part in the center and a mechanically robust fixed part in the edge. The fixed PCL part can improve the suture tension during surgery and bear interrupted suture in routine surgery. Moreover, Col−PCL membranes could facilitate HCEC adhesion, proliferation, and migration in vitro. Therefore, the prepared Col−PCL membranes dramatically increase the choice of artificial corneal grafts for the regeneration of cornea.

4. MATERIALS AND METHODS

4.1. Materials. Collagen extracted from bovine tendon was supplied by Pudao Lianxin Biotech, Co., Ltd. (Guangzhou, China). PCL (M_w 40 kDa) was purchased from Haishan Technology Co., Ltd. (Wuhan, China). The CCK-8 kit was purchased from Dojindo Laboratories (Japan). Fetal bovine serum (FBS), phosphate-buffered saline (PBS, pH = 7.4), and Dulbecco's modified Eagle's medium (DMEM)-basic (1×) was provided from Gibco. *N*-(3-Dimethylaminopropyl)-*N*′-ethylcarbodiimide hydrochloride (≥98.0%) (EDC) and *N*-hydroxysuccinimide (98.0%) (NHS) was purchased from Sigma-Aldrich (Shanghai, China). Collagenase I from clostridium histolyticum was supplied by QiYun Biotechnology Co., Ltd. (Guangzhou, China). Sodium fluorescein ophthalmic test papers were purchased from Tianjin Jingming New Technology Development Co., Ltd. (China, Tianjin). All other chemical reagents were of analytical grade and obtained from commercial sources.

4.2. Preparation of Col and Col−PCL Membranes. Col membranes were prepared as described in a previously published protocol.[53] In short, the crosslinking agents EDC and NHS were added to 6.5 mg/mL Col solution in 0.01 M HCl with a mass ratio of Col/(EDC/NHS) = 6:1 and stirred slowly at 4 °C for 8 h, in which the molar ratio of EDC to NHS was 4 to 1. After fully crosslinking, the homogeneous mixture was returned to room temperature and centrifuged to remove bubbles, following which the resulting mixture was poured into a disposable culture dish and air-dried in a clean bench. After washing, the air-dried membranes were put into a vacuum drying oven for thermal crosslinking. In this study, EDC/NHS is used to activate the carbonyl group when an amide bond is formed and generate synthetic crosslinks that form a bridge between amino acids without affecting any chemistry to the collagen molecule.[54] The preparation process of Col−PCL membranes is shown in Figure 1. Briefly, Col from fresh bovine tendon was dissolved in 0.01 M HCl solution at 4 °C, and the final concentration of Col was determined to be 6.5 mg/mL. The formed Col solution was then crosslinked by EDC and NHS, in which the molar ratio for the EDC to NHS was 4:1, and the Col to EDC/NHS mass ratio was 6:1. The EDC-mediated coupling reaction proceeded at 4 °C with stirring for 8 h. After the reaction was complete, the resulting mixture was placed at room temperature for 4 h and then centrifuged to remove bubbles. Immediately, the precursor solution was dispensed into a disposable culture dish and air-dried in a clean bench. PCL rings (outer diameter, 10 mm; inner diameter, 5 mm; thickness, 30−50 μm) were obtained by dissolution with dichloromethane, air drying, and tailoring. The obtained PCL ring was pressed into a part of the precursor solution until Col−PCL membranes are formed by air drying. The obtained Col and Col−PCL membranes were rinsed with deionized water five times to remove salt from the membrane. After the membranes were air-dried again, they were then put into a specific mold and hot-pressed in a vacuum drying oven for 24

DOI: 10.1021/acsomega.9b03297
ACS Omega 2020, 5, 674−682

h at 120 °C.[55] The obtained Col and Col−PCL membranes were stored in a desiccator for further characterization.

4.3. Macroscopic and Microscopic Morphology of the Membranes. The macroscopic morphology of the membranes was obtained by a digital camera, and the hierarchical structure was imaged using field-emission scanning electron microscopy (Philips Electronics N.V. Holland, SEM). Prior to the observation, the prepared membrane was quickly fractured in liquid nitrogen to observe the sectional morphology; the formed cross-section was then sputter-coated with platinum for observation.

4.4. Physical Characterization. Following immersion in normal saline (NS) for 2.5 h, transparency of the dry and wet membranes was determined by an ultraviolet−visible spectrophotometer (UNICO, China) at room temperature with the spectral range from 380 to 780 nm.

Water saturation was determined by the weight of the membranes and absorbed NS at different time points. Considering the small mass of the membranes, three homologous membranes were set to a sample and each batch was performed in triplicate. The equilibrated water content of the membranes was measured by the following steps. First, the membranes were weighed (W_0) and immersed in NS for 24 h at 37 °C. Subsequently, the membranes were taken out from the NS and the superficial NS was removed with filter papers and then weighed (W). The swelling ratio and water adsorption of the membranes were determined using the following equations

$$\text{swelling ratio } (\%) = (W - W_0)/W_0 \times 100\% \quad (1)$$

$$\text{water adsorption } (\%) = (W - W_0)/W \times 100\% \quad (2)$$

Tensile testing was performed on materials using DMA (Instron Corporation, Issaquah, WA) with a load velocity of 0.05 mm/s. In this study, the suture tension during surgery was simulated. To be brief, in the symmetrical position of the membranes, 10.0 suture was used to sew in the designated position, and then clamped in the fixture to pull. The maximum tension of the membrane is recorded.

4.5. In Vitro Degradation Experiment. Considering the weight of the membranes, two membranes with a diameter of 10 mm were defined as a sample. After samples (W_0) and 70 μm cell filters (W_1) were weighed respectively, the samples were put into the cell filters, and then the cell filters with samples were placed in collagenase type I solution (0.017 ng/mL). The cell filters with samples were removed from collagenase type I solution every 8 h, dried with filter paper, and weighed (W_2). The residual quality of samples in collagenase type I solution was calculated by the following equations

$$\text{membrane quality} = W_2 - W_1 - W_0 \quad (3)$$

4.6. Cell Proliferation and Adhesion Assay. Cell proliferation onto the membranes was assessed by the CCK-8 kit. Briefly, the samples sterilized by UV were put into sterile 48-well plates with DMEM-basic (1×) for 4 h and pressed into the bottom of well plates by sterile rubber rings to prevent it from floating in the liquid. Immediately after removing DMEM-basic (1×), HCECs (5×10^3) were seeded per sample and incubated in DMEM-basic (1×) supplemented with 10% FBS and 1% penicillin/streptomycin. The proliferative capacity was determined at day 1, 3, and 5. After adding CCK-8 reagent for 4 h, the absorbance of the collected supernatant medium at 450 nm was tested with a microplate reader (Thermo 3001, America).

Similarly, HCECs were seeded per sample and incubated for 24 h to evaluate cell adhesion on the samples. The CCK-8 assay on the basis of the manufacturer's instruction was used for quantitative analysis of the samples. In short, the surface of samples with HCECs was rinsed with PBS thrice after incubation for 24 h. Like cell proliferation, the samples with HCECs were incubated with the CCK-8 reagent for 4 h, and the absorbance of the collected supernatant at 450 nm was measured by a microplate reader. In addition, the samples with HCECs were rinsed with PBS thrice and immobilized with 2.5% polyformaldehyde (v/v) for 30 min at 4 °C, followed by sequential dehydration and drying. The samples were sputter-coated with platinum, and the cell status and morphology adhered to the sample were assessed using SEM.

4.7. Determination of Cell Viability. The calcein acetoxymethyl (calcein-AM)/(propidium iodide) PI double stain kit (Dojindo Laboratories, Japan) was employed to determine the viability of HCECs on the membranes for 5 days.[56] Briefly, calcein-AM (2 μmol/L) was diluted in absolute DMSO and PI (4 μmol/L) was diluted in ddH_2O to form the staining solution. Col, Col−PCL, and PCL membranes of 10 mm diameter were placed into 48-well plates. HCECs were seeded onto the surface of the membranes at a density of 1×10^4 cells per membrane ($n = 3$). Cells seeded at similar density on tissue culture plastic served as a control. After incubation at 37 °C for 5 days, cell medium was removed from wells and then the wells were rinsed with PBS thrice. Immediately after adding 100 μL of staining solution, cell-seeded membranes were incubated for 15 min at 37 °C, in the dark. After PBS washing, live (green stain) and dead (red stain) cells were imaged using a confocal laser scanning microscope (Leica TCS SP8). Finally, cell viability was quantified by the proportion of live cells to total cells, using ImageJ software.

4.8. Ex Vivo Cell Migration. All experimental procedures followed the Association for Research in Vision and Ophthalmology (ARVO) Statement that permits the Use of Animals in Ophthalmic and Vision Research, as well as the local ethical rules. Rabbit eyes were obtained from New Zealand white rabbits of euthanasia. Corneal grafts (Col−PCL membranes) of 7.25 mm diameter were surgically implanted into an isolated corneal anterior lamellar defect model (anterior wound diameter 7 mm). The samples were cultured in complete medium for 5 days. Re-epithelialization was tracked using sodium fluorescein ophthalmic test papers.

4.9. Statistical Analysis. Samples of at least $n = 3$ were used for data analysis. All data were presented as means ± standard deviations and statistical difference (p value) and analyzed using one-way analysis of variance. $p < 0.05$ was defined as statistically significant and marked with an asterisk.

AUTHOR INFORMATION

Corresponding Authors

*E-mail: phsongwj@scut.edu.cn (W.S.).
*E-mail: psliren@scut.edu.cn (L.R.).

ORCID

Wenjing Song: 0000-0003-4286-4512
Li Ren: 0000-0003-0604-9166

Author Contributions

Throughout the study, X.S. was responsible for all of the processes, including the study design, the collection, analysis,

DOI: 10.1021/acsomega.9b03297
ACS Omega 2020, 5, 674−682

or interpretation of data. X.S., W.S., and L.R. designed the study. X.Y. contributed to the preparation of materials. All authors have substantially contributed to the study and have given approval to the final version of the manuscript.

Notes

The authors declare no competing financial interest.

■ ACKNOWLEDGMENTS

This work was supported by the National Key R&D Program of China (2017YFC1105000 and 2018YFC0311103), the National Natural Science Foundation of China (51232002 and 51603073), the Guangdong Scientific and Technological Project (2017A030313294), the Pearl River S&T Nova Program of Guangzhou (201710010195), and the Guangzhou Regenerative Medicine and Health Guangdong Provincial Laboratory of the Basic Research and International Cooperation Department (2018GZR110105008).

■ REFERENCES

(1) Kong, B.; Sun, W.; Chen, G.; Tang, S.; Li, M.; Shao, Z.; Mi, S. Tissue-engineered cornea constructed with compressed collagen and laser-perforated electrospun mat. *Sci. Rep.* **2017**, *7*, No. 970.

(2) Cabalag, M.; Wasiak, J.; Syed, Q.; Paul, E.; Hall, A.; Cleland, H. Early and late complications of ocular burn injuries. *J. Plast. Reconstr. Aesthet. Surg.* **2015**, *68*, 356−361.

(3) Gheorghe, A.; Pop, M.; Mrini, F.; Barac, R.; Vargau, I. Ocular surface reconstruction in limbal stem cell deficiency. *Rom. J. Ophthalmol.* **2016**, *60*, 2−5.

(4) Iyer, G.; Srinivasan, B.; Agarwal, S.; Tarigopula, A. Outcome of allo simple limbal epithelial transplantation (alloSLET) in the early stage of ocular chemical injury. *Br. J. Ophthalmol.* **2017**, *101*, 828−833.

(5) Bourne, R.; Flaxman, S.; Braithwaite, T.; Cicinelli, M.; Das, A.; Jonas, J.; Keeffe, J.; Kempen, J.; Leasher, J.; Limburg, H.; Naidoo, K.; Pesudovs, K.; Resnikoff, S.; Silvester, A.; Stevens, G.; Tahhan, N.; Wong, T.; Taylor, H. Magnitude, temporal trends, and projections of the global prevalence of blindness and distance and bear vision impairment: a systematic review and meta-analysis. *Lancet Glob. Health* **2017**, *5*, e888−e897.

(6) Li, J.; Yu, L.; Deng, Z.; Wang, L.; Sun, L.; Ma, H.; Chen, W. Deep anterior lamellar keratoplasty using acellular corneal tissue for prevention of allograft rejection in high-risk corneas. *Am. J. Ophthalmol.* **2011**, *152*, 762−770.

(7) MacIntyre, R.; Chow, S.; Chan, E.; Poon, A. Long-term outcomes of deep anterior lamellar keratoplasty versus penetrating keratoplasty in australian keratoconus patients. *Cornea* **2014**, *33*, 6−9.

(8) Lagali, N.; Fagerholm, P.; Griffith, M. Biosynthetic corneas: prospects for supplementing the human donor cornea supply. *Expert Rev. Med. Devices* **2011**, *8*, 127−130.

(9) Long, K.; Liu, Y.; Li, W.; Wang, L.; Liu, S.; Wang, Y.; Wang, Z.; Ren, L. Improving the mechanical properties of collagen-based membranes using silk fibroin for corneal tissue engineering. *J. Biomed. Mater. Res., Part A* **2015**, *103*, 1159−1168.

(10) Ma, X.; Zhang, Y.; Zhu, D.; Lu, Y.; Zhou, G.; Liu, W.; Cao, Y.; Zhang, W. Corneal stroma regeneration with acellular corneal stroma sheets and keratocytes in a rabbit model. *PLoS One* **2015**, *10*, No. e0132705.

(11) Zhang, L.; Anderson, M.; Liu, C. The role of corneal stroma: a potential nutritional source for the cornea. *J. Nat. Sci.* **2017**, *3*, No. e428.

(12) Bueno, J. M.; Ávila, F. J.; Martínez-García, M. Quantitative analysis of the corneal collagen distribution after *in vivo* cross-linking with second harmonic microscopy. *Biomed. Res. Int.* **2019**, No. 3860498.

(13) Zhao, X.; Song, W.; Chen, Y.; Liu, S.; Ren, L. Collagen-based materials combined with microRNA for repairing cornea wounds and inhibiting scar formation. *Biomater. Sci.* **2019**, *7*, 51−62.

(14) Tsai, I.; Hsu, C.; Hung, K.; Chang, C.; Cheng, Y. Applications of biomaterials in corneal wound healing. *J. Chin. Med. Assoc.* **2015**, *78*, 212−217.

(15) Li, L.; Lu, C.; Wang, L.; Chen, M.; White, J.; Hao, X.; McLean, K.; Chen, H.; Hughes, T. Gelatin-based photocurable hydrogels for corneal wound repair. *ACS Appl. Mater. Interfaces* **2018**, *10*, 13283−13292.

(16) Liu, Y.; Liu, X.; Wu, M.; Ji, P.; Lv, H.; Deng, L. A collagen film with micro-rough surface can promote the corneal epithelization process for corneal repair. *Int. J. Biol. Macromol.* **2019**, *121*, 233−238.

(17) Liu, Y.; Ren, L.; Long, K.; Wang, L.; Wang, Y. Preparation and characterization of a novel tobramycin-containing antibacterial collagen film for corneal tissue engineering. *Acta Biomater.* **2014**, *10*, 289−299.

(18) Rose, J. B.; Sidney, L. E.; Patient, J.; White, L. J.; Dua, H. S.; El Haj, A. J.; Hopkinson, A.; Rose, F. R. A. J. *In vitro* evaluation of electrospun blends of gelatin and PCL for application as a partial thickness corneal graft. *J. Biomed. Mater. Res., Part A* **2019**, *107*, 828−838.

(19) de. la Mata, A.; Mateos-Timoneda, M.; Nieto-Miguel, T.; Galindo, S.; Lopez-Paniagua, M.; Planell, J.; Engel, E.; Calonge, M. Poly-L/DL-lactic acid films functionalized with collagen IV as carrier substrata for corneal epithelial stem cells. *Colloids Surf., B* **2019**, *177*, 121−129.

(20) Sun, X.; Wang, J.; Wang, Y.; Huang, C.; Yang, C.; Chen, M.; Chen, L.; Zhang, Q. Scaffold with orientated microtubule structure containing polylysine-heparin sodium nanoparticles for the controlled release of TGF-β1 in cartilage tissue engineering. *ACS Appl. Bio Mater.* **2018**, *1*, 2030−2040.

(21) Sun, X.; Wang, J.; Wang, Y.; Zhang, Q. Collagen-based porous scaffolds containing PLGA microspheres for controlled kartogenin release in cartilage tissue engineering. *Artif. Cells, Nanomed., Biotechnol.* **2017**, *46*, 1957−1966.

(22) Wang, J.; Sun, X.; Zhang, Z.; Wang, Y.; Huang, C.; Yang, C.; Liu, L.; Zhang, Q. Silk fibroin/collagen/hyaluronic acid scaffold incorporating pilose antler polypeptides microspheres for cartilage tissue engineering. *Mater. Sci. Eng., C* **2019**, *94*, 35−44.

(23) Wang, J.; Sun, X.; Cheng, N.; Wang, Y.; Huang, C.; Chen, M.; Liu, C.; Yang, C.; Zhang, Q. *In vitro* and *in vivo* studies of a collagen-based scaffold carrying PLGA microspheres for sustained release of epidermal growth factor in skin regeneration. *J. Biomater. Tissue Eng.* **2017**, *7*, 1336−1343.

(24) Mobaraki, M.; Abbasi, R.; Vandchali, S.; Ghaffari, M.; Mortarzadeh, F.; Mozafari, M. Corneal repair and regeneration: current concepts and future directions. *Front. Bioeng. Biotechnol.* **2019**, *7*, No. 135.

(25) Liu, Y.; Ren, L.; Wang, Y. Crosslinked collagen-gelatin-hyaluronic acid biomimetic film for cornea tissue engineering applications. *Mater. Sci. Eng., C* **2013**, *33*, 196−201.

(26) Liu, Y.; Ren, L.; Yao, H.; Wang, Y. Collagen films with suitable physical properties and biocompatibility for corneal tissue engineering prepared by ion leaching technique. *Mater. Lett.* **2012**, *87*, 1−4.

(27) Rajzer, I.; Dziadek, M.; Kurowska, A.; Cholewa-Kowalska, K.; Zibka, M.; Menaszek, E.; Douglas, T. Electrospun polycaprolactone membranes with Zn-doped bioglass for nasal tissues treatment. *J. Mater. Sci. Mater. Med.* **2019**, *30*, 80.

(28) Babaloo, H.; Ebrahimi-Barough, S.; Derakhshan, M.; Yazdankhah, M.; Lotfibakhshaiesh, N.; Soleimani, M.; Joghataei, M.; Ai, J. PCL/gelatin nanofibrous scaffolds with human endometrial stem cells/schwann cells facilitate axon regeneration in spinal cord injury. *J. Cell. Physiol.* **2019**, *234*, 11060−11069.

(29) Idini, M.; Wieringa, P.; Rocchiccioli, S.; Nieddu, G.; Ucciferri, N.; Formato, M.; Lepedda, A.; Moroni, L. Glycosaminoglycan functionalization of electrospun scaffolds enhances schwann cell activity. *Acta Biomater.* **2019**, *96*, 188−202.

(30) Cheng, G.; Yin, C.; Tu, H.; Jiang, S.; Wang, Q.; Zhou, X.; Xing, X.; Xie, C.; Shi, X.; Du, Y.; Deng, H.; Li, Z. Controlled co-delivery of growth factors through layer-by-layer assembly of core-shell nano-

DOI: 10.1021/acsomega.9b03297
ACS Omega 2020, 5, 674−682

fibers for improving bone regeneration. *ACS Nano* **2019**, *13*, 6372−6382.
(31) Salehi, S.; Czugala, M.; Stafiej, P.; Fathi, M.; Bahners, T.; Gutmann, J.; Singer, B.; Fuchsluger, T. Poly (glycerol sebacate)-poly (epsilon-caprolactone) blend nanofibrous scaffold as intrinsic bio- and immunocompatible system for corneal repair. *Acta Biomater.* **2017**, *50*, 370−380.
(32) Park, Y.; Cha, J.; Bang, S.; Kim, S. Clinical application of three-dimensionally printed biomaterial polycaprolactone (PCL) in augmentation rhinoplasty. *Aesthetic Plast. Surg.* **2019**, *43*, 437−446.
(33) Balagangadharan, K.; Trivedi, R.; Vairamani, M.; Selvamurugan, N. Sinapic acid-loaded chitosan nanoparticles in polycaprolactone electrospun fibers for bone regeneration *in vitro* and *in vivo*. *Carbohydr. Polym.* **2019**, *216*, 1−16.
(34) Chen, X.; Zhang, Q.; Hou, D.; Lin, J.; Gao, J.; Wang, L. Fabrication and characterization of novel antibacterial silk sutures with different braiding parameters. *J. Nat. Fibers* **2019**, *16*, 866−876.
(35) El-Bakary, M. A.; El-Farahaty, K. A.; El-Sayed, N. M. Investigating the mechanical behavior of PGA/PCL copolymer surgical suture material using multiple-beam interference microscopy. *Fiber Polym.* **2019**, *20*, 1116−1124.
(36) Ghodbane, S. A.; Patel, J. M.; Brzezinski, A.; Lu, T. M.; Gatt, C. J.; Dunn, M. G. Biomechanical characterization of a novel collagen-hyaluronan infused 3D-printed polymeric device for partial meniscus replacement. *J. Biomed. Mater. Res., Part B* **2019**, *107*, 2457−2465.
(37) Hu, J.; Zhou, Y.; Huang, L.; Lu, H. Development of biodegradable polycaprolactone film as an internal fixation material to enhance tendon repair: an *in vitro* study. *BMC Musculoskeletal Disord.* **2013**, *14*, No. 246.
(38) Zhao, H.; Ma, L.; Gao, C.; Shen, J. A composite scaffold of PLGA microspheres/fibrin gel for cartilage tissue engineering: fabrication, physical properties, and cell responsiveness. *J. Biomed. Mater. Res., Part B* **2009**, *88B*, 240−249.
(39) Fagerholm, P.; Lagali, N.; Merrett, K.; Jackson, W.; Munger, R.; Liu, Y.; Polarek, J.; Soderqvist, M.; Griffith, M. A biosynthetic alternative to human donor tissue for inducing corneal regeneration: 24-month follow-up of a phase 1 clinical study. *Sci. Transl. Med.* **2010**, *2*, No. 46ra61.
(40) Samarawickrama, C.; Samanta, A.; Liszka, A.; Fagerholm, P.; Buznyk, O.; Griffith, M.; Allan, B. Collagen-based fillers as alternatives to cyanoacrylate glue for the sealing of large corneal perforations. *Cornea* **2018**, *37*, 609−616.
(41) Kim, H.; Jang, J.; Park, J.; Lee, K.; Lee, S.; Lee, D.; Kim, K.; Kim, H.; Cho, D. Shear-induced alignment of collagen fibrils using 3D cell printing for corneal stroma tissue engineering. *Biofabrication* **2019**, *11*, No. 035017.
(42) Kilic Bektas, C.; Hasirci, V. Mimicking corneal stroma using keratocyte loaded photopolymerizable methacrylated gelatin hydrogels. *J. Tissue. Eng. Regen. Med.* **2018**, *12*, e1899−e1910.
(43) van den Berg, T. J.; Tan, K. E. Light transmittance of the human cornea from 320 to 700 nm for different ages. *Vision Res.* **1994**, *34*, 1453−1456.
(44) Aghaei-Ghareh-Bolagh, B.; Guan, J.; Wang, Y.; Martin, A.; Dawson, R.; Mithieux, S.; Weiss, A. Optically robust, highly permeable and elastic protein films that support dual cornea cell types. *Biomaterials* **2019**, *188*, 50−62.
(45) Majumdar, S.; Wang, X.; Sommerfeld, S.; Chae, J.; Athanasopoulou, E.; Shores, L.; Duan, X.; Amzel, L.; Stellacci, F.; Schein, O.; Guo, Q.; Singh, A.; Elisseeff, J. Cyclodextrin modulated type I collagen self-assembly to engineer biomimetic cornea implants. *Adv. Funct. Mater.* **2018**, *28*, No. 1804076.
(46) Liu, W.; Deng, C.; McLaughlin, C.; Fagerholm, P.; Lagali, N.; Heyne, B.; Scaiano, J.; Watsky, M.; Kato, Y.; Munger, R.; Shinozaki, N.; Li, F.; Griffith, M. Collagen-phosphorylcholine interpenetrating network hydrogels as corneal substitutes. *Biomaterials* **2009**, *30*, 1551−1559.
(47) Bhattacharjee, P.; Fernandez-Perez, J.; Ahearne, M. Potential for combined delivery of riboflavin and all-trans retinoic acid, from silk fibroin for corneal bioengineering. *Mater. Sci. Eng., C* **2019**, *105*, No. 110093.
(48) Zieske, J. Extracellular matrix and wound healing. *Curr. Opin. Ophthalmol.* **2001**, *12*, 237−241.
(49) Suárez-Barrio, C.; Etxebarria, J.; Hernaez-Moya, R.; del Val-Alonso, M.; Rodriguez-Astigarraga, M.; Urkaregi, A.; Freire, V.; Morales, M.; Duran, J.; Vicario, M.; Molina, I.; Herrero-Vanrell, R.; Andollo, N. Hyaluronic Acid Combined with Serum Rich in Growth Factors in Corneal Epithelial Defects. *Int. J. Mol. Sci.* **2019**, *20*, 1655.
(50) Bohnsack, R. N.; Warejcka, D. J.; Wang, L.; Gillespie, S. R.; Bernstein, A. M.; Twining, S. S.; Dahms, N. M. Expression of insulin-like growth factor 2 receptor in corneal keratocytes during differentiation and in response to wound healing. *Invest. Ophthalmol. Visual Sci.* **2014**, *55*, 7697−7708.
(51) Deshpande, P.; Ortega, I.; Sefat, F.; Sangwan, V.-S.; Green, N.; Claeyssens, F.; MacNeil, S. Rocking media over *ex vivo* corneas improves this model and allows the study of the effect of proinflammatory cytokines on wound healing. *Invest. Ophthalmol. Visual Sci.* **2015**, *56*, 1553−1561.
(52) Pinheiro, R.; Panfil, C.; Schrage, N.; Dutescu, R. M. The impact of glaucoma medications on corneal wound healing. *J. Glaucoma* **2016**, *25*, 122−127.
(53) Zhao, X.; Liu, Y.; Li, W.; Long, K.; Wang, L.; Liu, S.; Wang, Y.; Ren, L. Collagen based film with well epithelial and stromal regeneration as corneal repair materials: improving mechanical property by crosslinking with citric Acid. *Mater. Sci. Eng., C* **2015**, *55*, 201−208.
(54) Nong, L.; Zhou, D.; Zheng, D.; Jiang, Y.; Xu, N.; Zhao, G.; Wei, H.; Zhou, S.; Han, H.; Han, L. The effect of different cross-linking conditions of EDC/NHS on type II collagen scaffolds: an *in vitro* evaluation. *Cell Tissue Banking* **2019**, 557.
(55) Ueda, H.; Hong, L.; Yamamoto, M.; Shigeno, K.; Inoue, M.; Toba, T.; Yoshitani, M.; Nakamura, T.; Tabata, Y.; Shimizu, Y. Use of collagen sponge incorporating transforming growth factor-b1 to promote bone repair in skull defects in rabbits. *Biomaterials* **2002**, *23*, 1003−1010.
(56) Sani, E.; Kheirkhah, A.; Rana, D.; Sun, Z.; Foulsham, W.; Sheikhi, A.; Khademhosseini, A.; Dana, R.; Annabi, N. Sutureless repair of corneal injuries using naturally derived bioadhesive hydrogels. *Sci. Adv.* **2019**, *5*, No. eaav1281.

DOI: 10.1021/acsomega.9b03297
ACS Omega 2020, 5, 674−682